3D vector approach to local thermally driven slope winds modeling

Alfonso Vitti , Paolo Zatelli , Fabio Zottele

Department of Department of Civil and Environmental Engineering, via Mesiano 77, 38100 Trento, Italy, tel +390461882618, fax +390461882672, e-mail Paolo.Zatelli@ing.unitn.it

Abstract

A vector model has been setup to evaluate wind speed and direction for thermally driven slope winds. This model is based on an extension of the Prandtl model and uses the new GRASS 3D vector implementation as well as its connection to external DBMS. This model follows the model for the raster approach to a local metereological model for the evaluation of temperature, wind speed and humidity [1], based on the 3D raster GRASS capability. The new vector implementation allows the evaluation of temperature, wind speed and direction on a set of irregular placed points, while the raster approach is constrained to use points on a regular grid. Moreover, all the attributes that are used as parameters in the model are managed through PostgreSQL and SQL queries. A new GRASS module has been written to evaluate the normal direction through a point in the 3D space, since all the model parameters depend on the distance from the surface along the normal direction. A comparison between the vector and the raster approach, in terms of implementation and use, is presented. Finally a synthetic and a real simulation and a comparison with the raster model results are reported.

1 Introduction

The integration of environmental models and GIS is driven by the effort towards the development of a comprehensive description of a system, where each interrelated factor can be correlated by its position in the space. Infact, the management of hetherogeneus data linked by their position is what GISs are about.

The development of a model for local atmospheric study within a GIS environment has started some years ago, resulting in a local thermally driven slope winds model based on the 3D raster GRASS model [1], [2], [3]. This model evaluates wind velocity and (potential) temperature anomaly in a volume over a slope.

The (3D) raster approach implies that, while it possible to choose the resolution along the three axes, the variables must be estimated over the whole domain. Since heavy geometric calculation is involved for the determination of the normal direction to the terrain surface, this can be needless burdensome when the values in only a small set of point are needed. For example the model has been tested matching its output against the measurement taken by a motor glide in the Adige valley, about 2 *km* wide, with an entire track about 15 *km* long and 2 *km* high [4]. The total air volume involved in the measurements is about 60 km^3, therefore a discretization with 10x10x10 meters voxels implies 60 millions of cells.

A vector approach, where wind velocity and (potential) temperature anomaly can be evaluated on an arbitrary set of points, makes the matching between simulated and measured values feasible since it is sufficient to perform the calculations only on the glide trajectory, which is determined by GPS.

Therefore, the first goal of this work is to implement all the geometric part of the model following a vector approach. Moreover, the application of the model can be made faster and more easily manageable if all the non geometric (semantic) part of the model is stored and managed by a database management system, linked to geometric data.

A side purpose of this work is the testing of the new GRASS vector model both from the user and from the programmer perspective.

2 Thermally drive slope winds

The diurnal cycle of incoming solar radiation and outgoing longwave radiation at night determines a cyclical heating and cooling of the air layers closer to the ground, causing airflows along sloping terrains. These slope winds are more relevant in mountain valleys, where the temperature gradients due to the mountain slopes influence the lower air layers and the whole air motion inside a valley is affected [7].

The theoretical formulation for thermally induced flows on a slope has been provided by Prandtl [6], confirmed by the sperimental work of Defant [5]. A sloping ground is modeled by a tilted plane, with an angle α with respect to the horizontal, while the atmosphere above is unperturbed and stable. Two reference frames are usually established: one is the usual Cartesian reference, with the direction *x* along the slope on the horizontal plane and *z* in the vertical direction, the second one has a coordinate *s* along the slope and *n* normal to it (see figure 1).

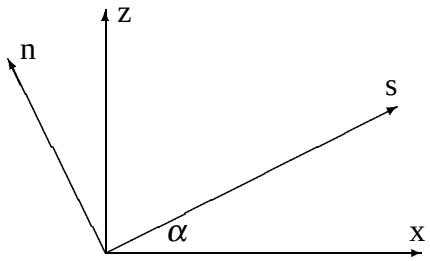

Figure 1: Reference systems on the tilted plan modeling the sloping ground.

Air movements and temperature distribution are due to the heat fluxes the air volume is exposed to. The main energy source is the solar radiation, this energy is partly reflected back to the air by the terrain surface and partly adsorbed by the ground; this latter part is in turn divided in heat flux into the ground and sensible or latent heat flux conveyed back to the air layers closer to the surface.

Indicating as positive the heat fluxes from the ground to the atmosphere, the heat budget can be written as

$$-Q_S^* = Q_H + Q_E - Q_G \tag{1}$$

where Q_S^* is the net solar radiation flux, Q_H the sensible heat flux, Q_E the latent heat flux and Q_G the ground heat flux. The incoming net radiation flux Q_S^* is evaluated as a fraction of the extraterrestrial solar radiance, taking into account reflection and absorption by the atmosphere, and the ground flux Q_G is estimated as a fraction of the net radiation flux Q_S^* by

$$Q_G = aQ_S^* \tag{2}$$

where the coefficient *a* ranges from 0.1 for the daytime to 0.5 for the nighttime. A simpler formulation sets this ratio to 3/10

$$Q_G = 0.3\, Q_S^* \tag{3}$$

Sensible heat flux and latent heat flux are estimated by closing the budget equation, after having chosen a proper ratio between the two, the so called Bowen ratio coefficient β_R

$$\beta_R = \frac{Q_H}{Q_E} \tag{4}$$

A more detailed discussion of the determination of these heat fluxes can be found in [1], [2], [3], where references are provided.

The evaluation of the the sensible heat flux Q_H is essential for the estimation of temperature and wind velocity over the slope. Rather than to absolute temperature, heat exchange is related to *potential temperature*, that is the temperature that an air parcel volume would have if led to a reference pressure (usually 1000 hPa) along an adiabatic transformation. The link between absolute T and potential θ temperature is given by the well known Poisson equation

$$\theta = T\left(\frac{p_0}{p}\right)^{\frac{R_d}{c_p}} \tag{5}$$

where p is the atmospheric pressure, p_0 is the reference pressure, $R_d = 287\ JK^{-1}kg^{-1}$ the gas constant for dry air and $c_p = 1004\ JK^{-1}kg^{-1}$ is the specific heat at constant pressure. Heating and cooling of the

ground impart an anomaly $\Delta\theta$ on the potential temperature, which in an unperturbed atmosphere shows a positive gradient

$$\theta = A + \Gamma z + \Delta\theta\,(n) \tag{6}$$

where z is the vertical coordinate and n the normal coordinate to the slope (see figure 1), Γ is the potential temperature vertical gradient in standard atmospheric conditions and A an integration constant (i.e. the temperature at soil level). The anomaly of potential temperature $\Delta\theta$ can be written as

$$\Delta\theta = Ce^{-\frac{n}{l}}\cos\left(\frac{n}{l}\right) \tag{7}$$

where C is the potential temperature anomaly at ground level, and l is the typical length scale of the phenomenon

$$l = \sqrt[4]{\frac{4\nu_H\nu_k}{g\beta\Gamma\sin\alpha}} \tag{8}$$

where, again, ν_H is the air thermal diffusivity, ν_k is the air kinematic viscosity, g the gravity acceleration, $\beta = 273.15^{-1}$ and α the slope angle.

These same parameters can be used to estimate the wind velocity component along the slope

$$u = C\sqrt{\frac{g\beta\nu_H}{\Gamma\nu_k}}e^{-\frac{n}{l}}\sin\left(\frac{n}{l}\right) \tag{9}$$

The value of the integration constant C can be evaluated by imposing the boundary condition at the ground-atmosphere interface that the (potential) temperature variation in the n direction is proportional to the sensible heat flux Q_H, as expressed by the Fourier law

$$Q_H = -k_H \left.\frac{\partial\Delta\theta}{\partial n}\right|_{n=0} \tag{10}$$

where k_H is the air thermal conductivity; the potential temperature anomaly variation along the s coordinate can be neglected if the motion is uniform along the slope. By substituting equation 7 in 10, C can be expressed as

$$C = \frac{Q_H l}{k_H} \tag{11}$$

It is possible to take into account the effects of water vapor, modifying the Prandtl's model, by introducing the virtual potential temperature θ_V

$$\theta_V = (1 + 0.61q)\,T\left(\frac{p_o}{p}\right)^{\frac{R_d}{c_p}} = \theta\,(1 + 0.61q) \tag{12}$$

where q is the specific humidity. The expressions for θ_V and u can be derived by applying the same procedure above, but in addition to the heat budget condition of equation 1 the conservation of moisture flux F_W must be imposed [2].

3 GIS procedure

As seen in the previous section, the evaluation of (potential) temperature anomaly and wind velocity along a slope requires the knowledge of the sensible heat flux on the surface and of the distance of the point from the surface itself, along the normal direction.

The sensible heat flux can be evaluated from the incidence angle between solar beams direction and the normal to the surface, the atmosphere features and the land cover. The incidence angle can be easily determined in GRASS by the `r.sun` module. The relevant atmospheric parameters are the absorption, reflection and transmission coefficients, the atmospheric transmissivity and the cloud cover factor. The land cover influence is taken into account by the albedo, soil thermal capacity and, for vegetation cover, leaf

resistance to vapor flux. All these parameters must be available as geographically referenced information, so that their combination to evaluate the sensible heat flux is possible. In the raster approach each parameter is represented by a raster 2D map on the terrain or a set of atmospheric parameters, in the vector approach the parameters are stored in a database and linked dynamically to the (vector) geometry.

The only raster map is the digital terrain model (DTM), but a vector DTM such as a TIN can be used, exploiting the new GRASS vector capabilities.

4 Evaluation of the normal to a surface

The terrain surface is expressed by a raster DTM and slope and aspect maps are easily evaluated. While the gradient components of the DTM would be more suitable for the determination of the normal direction though a point in the space, the wide availability of slope and aspect information makes these parameters preferable for this task.

The main problem in the individuation of the normal to a DTM through a point is that in general a DTM does not describe a simple geometric known surface, therefore it is not possible to write an explicit expression for the normal direction. The workaround comes from the observation that for points close to the surface the distance on the surface between *normal* and *vertical* projection is usually small, save for singular situations. The determination of the vertical projection on the surface is trivial and this point can be used as starting point for the search of the normal projection, which is the point corresponding to the minimum distance. The algorithm that evaluates the normal to a surface uses this proposition, starting from a point close to the surface and moving towards the interesting point.

Let $P\ (x_P,y_P,z_P)$ be the point to be projected and $V\ (x_V,y_V,z_V)$ the vertical projection on the surface, the segment $\overline{PV}$ is divided into k parts, each with edge points $P_V(i)$ with coordinates given by

$$P_V(i)(x_P - i\frac{\overline{PV}}{k}, y_P - i\frac{\overline{PV}}{k}, z_P - i\frac{\overline{PV}}{k}) \tag{13}$$

with i running from 0 to k, where obviously $P_V(i) \equiv V$ for $i = 0$, $P_V(i) \equiv P$ for $i = k$ and lower values of k correspond to points closer to the surface. The algorithm starts with $k = 1$, for this point $P_V(1)$, which is close to the terrain surface, the normal and vertical direction are close, unless the slope is very slanting or a singularity of the surface is involved. Therefore, a windows of points under $P_V(1)$ is scanned and the distances from $P_V(1)$ and the centers of all these cells are evaluated. Then the point $Q\ (x_Q,y_Q,z_Q)$ corresponding to the shortest distance $d_{min} = \overline{PQ}$ is selected.

The versor

$$\vec{\mathbf{v}}_Q = \frac{\overleftarrow{Q - P_V(1)}}{d_{min}} \tag{14}$$

identifies the direction of the segment from $P_V(1)$ to Q, which in general is not the normal direction since only the cell centers are tested. Still, it is possible to evaluate the normal direction to the terrain surface from the DTM gradient for the cell to which Q belongs. This is done by calculating the versor

$$\vec{\mathbf{v}}_{DTM} = \frac{\vec{\nabla}}{\|\nabla\|} = \frac{(\nabla_x, \nabla_y, \nabla_z)}{\sqrt{{\nabla_x}^2 + {\nabla_y}^2 + {\nabla_z}^2}} \tag{15}$$

If $\vec{\mathbf{v}}_Q = \vec{\mathbf{v}}_{DTM}$ then $\vec{\mathbf{v}}_Q$ is the normal direction through $P_V(1)$, otherwise, as usually happens, the distance from Q to the normal projection point N can be evaluated as follows:

$$d = |\vec{\mathbf{v}}_Q \cdot \vec{\mathbf{v}}_{DTM}|\ \|P - Q\| \tag{16}$$

and N is found by moving of d along the opposite direction of $\vec{\mathbf{v}}_{DTM}$

$$N = P - \vec{\mathbf{v}}_{DTM}\, d \tag{17}$$

Once the projection point N for $P_V(1)$ is found, the procedure is iterated for the other $k-1$ points. However, after the first iteration the point N of the previous iteration, rather than the vertical projection, is used as starting point for the search.

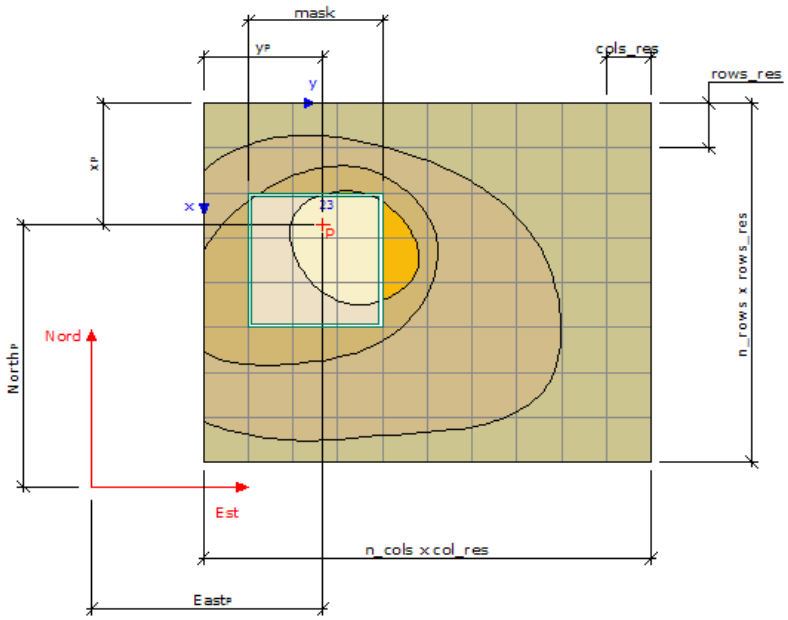

Figure 2: Scanning window over the DTM for the search of the minimum distance point.

The two parameters that must be chosen in this procedure are k, the number of segments into which the vertical segment from the point to the surface is divided, and m, the dimension, as number of cells in its side, of the square search window on the terrain. These parameters are set as a trade off between the risk of selecting the wrong point on the surface and the computational cost. Infact, the choice of large values for k increases the number of iteration of the procedure above, while small values of k can lead to situations in which the hypothesis that normal and vertical directions are close does not hold, resulting in the failure of the algorithm. The selection of large values of m causes the need of scanning a large number of cells when looking for the distance minimum (the number of scanned cells scales with m^2), however a small value of m can lead to the individuation of a *local* minimum for the cells' centers - point distances, which is not the real minimum, resulting again in a failure of the procedure.

Once the projection point N coordinates are known, it is possible to evaluate the distance of a point from the surface along the normal direction, i.e. calculate the n coordinate of section 2. Moreover, the address cell under the point in the normal direction is known, therefore the sensible heat flux can be evaluated.

5 Implementation

The algorithm describe in section 4 has been implemented as a new GRASS module `v.pep.seek`, taking advantage from the new GRASS vector architecture and the possibility of link to databases. The `v.pep.seek` module creates a tridimensional vector map of the segments that connect each input point with its projection on a DTM. To each segment a table is associated, storing the following information: the coordinates of the point to be projected, the coordinates of the projection point, the distance between these points, the indexes of the DTM cell containing the projection point and the coordinates of the baricenter of the cell. This module has been written to implement a model of local thermally driven slope winds, however it as been designed with a more generic use in mind: it solves the geometric part of the problem with no reference to the atmospheric model. For example, it is possible to evaluate the normal direction to a surface for points *below* the surface: while it makes no sense for the implementation of an atmospheric model, this can be used in other applications. The HTML manual of the module `v.perp.seek` is shown in figure 3.

The input of the modules consists in: a vector map containing the points whose normal must be evaluated and three raster maps representing the DTM, the slope (in degrees) and the aspect (in degrees), the latter two are used to evaluate the local gradient of the surface and can be easily created in GRASS using the `r.slope.aspect` module. For complex (concave) terrain morphologies it is possible that there exist

DESCRIPTION

v.perp.seek generates a 3D vector map of lines. Every line connects the point to be projected (wich is read from an input 3D vector file of points) and the normal projection on DTM, calculated by the module. In the linked table are stored several information above the projections: the coordinates of the point to be projected, the distance between the two points, the coordinates of the normal projection, the number of the cell whwr the projection falls, the two planimetric coordinates of the cell in which projection falls, the directions of the gradient versor and the components of the maximum slope direction. The user must specify:

1. the *3D vector file* for the points;
2. the input *elevation* file name;
3. the output file name;
4. the *slope file (degrees);*
5. the *aspect file (degrees).*

Moreover, the module needs to specify two further parameters:

- the number *trim* of slices to cut the line joining the point to project with his vertical projection on DTM into;
- the dimension *mask* of the neighborhood matrix containing DTM's points where the normal projection is iteratively computed.

The raster *elevation* map layer, specified by the user, must contain true elevation values, *not* rescaled or categorized data.
The raster *aspect* map layer indicates the direction that slopes are facing. The aspect categories represent the number degrees of east.
The raster *slope* map layer contains slope values, in degrees of inclination from the horizontal.

NOTES

The algorithm used to determine the normal projection is a "user set" neighborhood tool. The vertical projection is cut in several slices (set by user, too). The point elevated from the first slice, supposed to be rather near the DTM, is connected with each cell of the elevation file in the window. Thus, it is possible to determine the cell with the minimum distance. Collecting slope and aspect for that element, the module computes the components of gradient (Horn's formula) and finds the normal projection. Iteratively the projection is found for the next slice and so on, till the top of vertical projection (i.e. the point to be projected) is reached.

NULL cell or cell outside region are set to a defined value (-999.) avoiding errors on searching the projection.

WARNING

The module is still under testing.

REFERENCE

Vitti, Alfonso. Tesi di Laurea.*Modellazione tridimensionale mediante GIS-GRASS di venti di pendio forzati termicamente.*Università degli Studi di Trento. Facoltà di Ingegneria, Trento, 2002. The master thesis is available at "Biblioteca di Ingegneria", Trento, sign. 317.

SEE ALSO

r.slope.aspect

AUTHOR

Fabio Zottele. Università degli Studi di Trento

Last changed: $Date: 2004/05/20 23:55:02 $

Figure 3: `HTML` manual of the module `v.perp.seek`.

more than one normal, the modules select the direction corresponding to the shortest distance, since the variables (temperature and wind speed in our model) in one point are likely influenced more from closer points on the surface.

6 Tests

Before the application of the new module to the atmospheric model, some tests have been carried out to check its correct functioning. In the first set of tests, series of planes have been used to match the results of the use of the module against the analytic determination of the coordinates of the projection points and their distance from the projecting point. One of these tests uses the following plane

$$z = 75 - \frac{3}{4}x - \frac{1}{2}y = 75 - 0.75x - 0.5y \tag{18}$$

shown in figure 5. Points above and below the surface are projected.

The coordinates of the points to be projected $P\,(x_P, y_P, z_P)$, the coordinates of the theoric projected points $(x_{Nteor}, y_{Nteor}, z_{Nteor})$, the coordinates of the projected points estimated by the module (x_N, y_N, z_N) and their distances from P, theoric d_{teor} and evaluated by the module d, are shown in table 1.

The differences are very small, see table 2, and can be ascribed to numerical roundoff.

The database associated to each segment can be seen in figure 6.

Other experiments have been carried out for more complex surfaces such as those used with the raster approach in [1], [2] and [3]. One example is in figure 7. All the points in the volume above the surface have

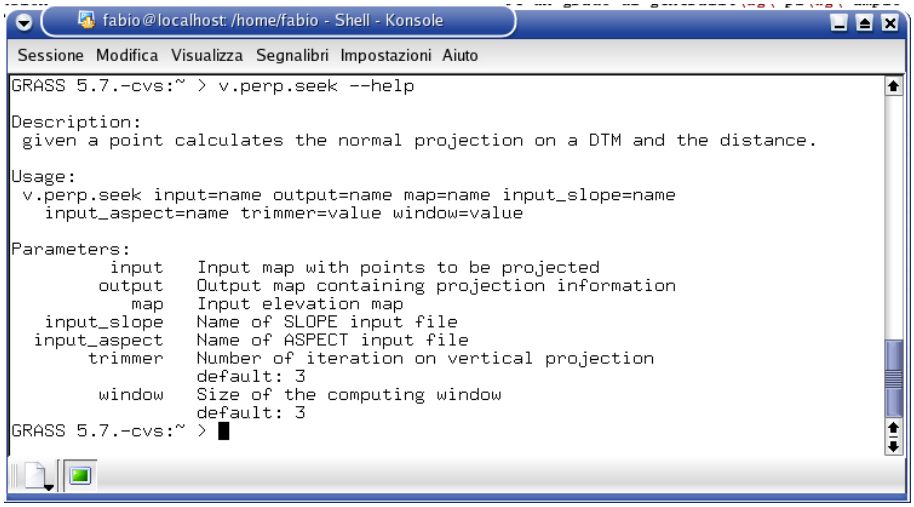

Figure 4: Console help of the module `v.perp.seek` showing its parameters.

point	x_P	y_P	z_P	d	x_N	y_N	z_N
1	37	73	50	29.154164	20.758617	62.172399	28.344844
2	32	25	90	38.253242	10.689646	10.793081	61.586222
3	70	34	100	70.192838	30.896537	7.930995	47.862099
4	50	50	-40	38.996023	71.724147	64.482781	-11.034498
point	x_P	y_P	z_P	d_{teor}	x_{Nteor}	y_{Nteor}	z_{Nteor}
1	37	73	50	29.15416809	20.75862069	62.17241379	28.34482758610
2	32	25	90	38.25323966	10.68965517	10.79310345	61.58620689641
3	70	34	100	70.19283783	30.89655172	7.931034483	47.86206896525
4	50	50	-40	38.99602102	71.72413793	64.48275862	-11.03448275847

Table 1: Comparison between theoric coordinates and distances and values estimated by `v.perp.seek`.

been projected, so that the comparison with the results of the `r3.isosurf` GRASS module, used for the cited papers, is possible. For every surface the results are identical, it is therefore possible to assert the good functioning of the module.

7 Applications

The first application is used as an overall test of the model. Infact, Defant's [5] conditions have been used to evaluate parameters that are matched against his sperimental data. According to Defant's measurement campaign the following conditions are chosen:

- planar slope;
- uniform solar coverage and irradiation;

point	$diff_{dist}$	$diff_{xN}$	$diff_{yN}$	$diff_{zN}$
1	-4.09E-06	-3.69E-06	-1.48E-05	1.64E-05
2	2.34E-06	-9.17E-06	-2.24E-05	1.51E-05
3	1.69E-07	-1.47E-05	-3.95E-05	3.00E-05
4	1.98E-06	9.07E-06	2.24E-05	-1.52E-05

Table 2: Differences for projected points coordinates and distances between theoric and estimated by the model `v.perp.seek` values.

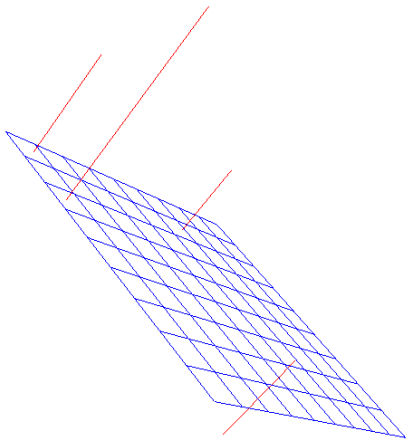

Figure 5: Projection of points on the plane $z = 75 - 0.75x - 0.5y$. One point is below the surface. The image is a `nviz` module snapshot.

- unperturbed and stratified atmosphere.

Table 3 shows the values of the constants and parameters used to solve equations 7 and 9.

Since the C parameter values in table 3 are valid only for the initial hours of the day or of the night, a new procedure has been setup for the evaluation of the C parameter on the slope, which uses the equations of section 2 and the sensible heat flux is evaluated by using the `r.sun` GRASS module. The output of this procedure is a 2D map of the value of C for a given hour of the day. Since the successive elaboration is made by manipulating database tables, this raster map is exported as a vector map with an associated table.

The wind velocity along the slope u and the potential temperature anomaly $\Delta\theta$ are evaluated with the following procedure:

- for each point the normal direction to the DTM surface is evaluated by the `v.perp.seek` module;
- for each point the value of C is read from the database table;
- equations 7 and 9 are solved using a SQL statement;
- the resulting table is associated to the input vector file containing the investigated points, replacing the original table.

All the database management is done by PostgreSQL via the `pg` GRASS driver, this allows great flexibility and overcomes the impossibility (at time of writing) of adding new fields to a table when using the internal `dbf` driver.

The GRASS commands used in this procedure are `db.copy`, `v.db.connect` and `v.category`, while the SQL query solving equations 7 and 9 is

```
CREATE TABLE wind
AS SELECT n.cat, (C.value*exp(-n.distance/34.4)*
*cos(n.distance/34.4))
AS delta_theta,
(C.value*sqrt(9.8/288*0.71/0.002)*exp(-n.distance/34.4)*
*sin(n.distance/34.4))
AS u,
(C.value*sqrt(9.8/288*0.71/0.002)*exp(-n.distance/34.4)*
*sin(n.distance/34.4)*n.wind_x)
```

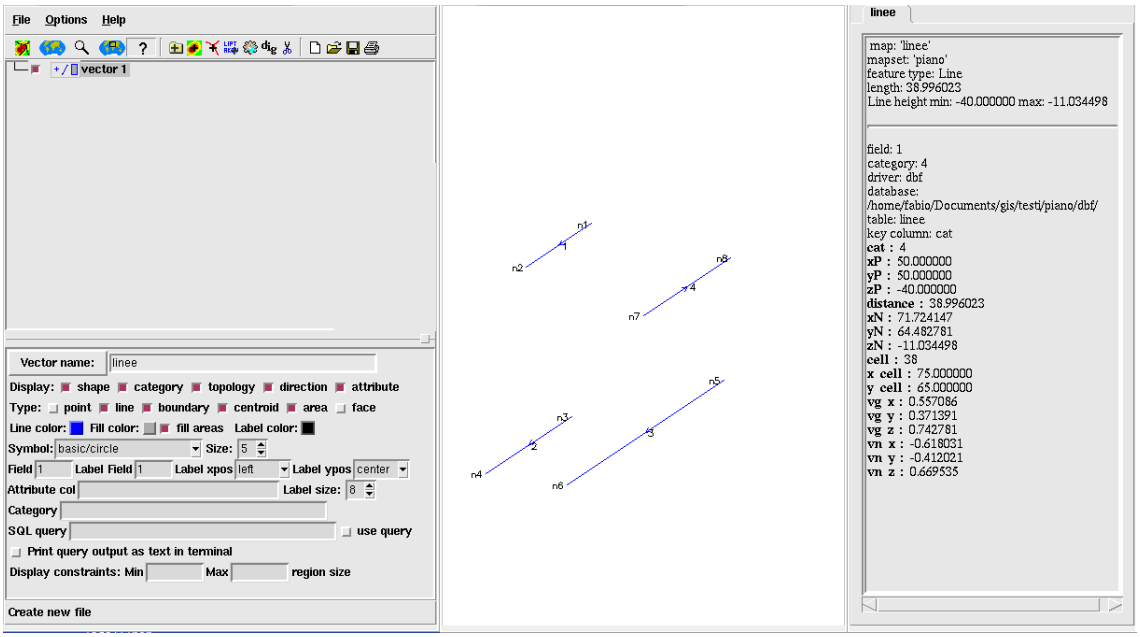

Figure 6: Output from the module `v.perp.seek`: attributes of one geometric feature (line) are shown on the right side.

```
AS ws_x,
(C.value*sqrt(9.8/288*0.71/0.002)*exp(-n.distance/34.4)*
*sin(n.distance/34.4)*n.wind_y)
AS ws_y,
(C.value*sqrt(9.8/288*0.71/0.002)*exp(-n.distance/34.4)*
*sin(n.distance/34.4)*n.wind_z)
AS ws_z
FROM n, C WHERE C.cat = n.cell;
```

The results of the application of the model match the sperimental measurement in [5], the outline of the temperature distribution in the day and at night is shown in figure 8.

Other applications have been carried out for real slopes near Trento. The output of the model for a slope near the village of Besenello, 10 km south Trento along the Adige valley are shown in figures 9-11.

The same slope has been investigated in [1], [2] and [3] with a raster approach: the comparison of the results in figures 12 and 13 shows a good agreement between the two solutions.

8 Vector vs raster approach

The comparison of raster and vector approaches can be done in terms of overall performance of the procedure, taking into account elaboration times, ease of data management and flexibility, and of efficiency for the implementation.

The implementation of the vector approach has suffered from the early stage of the GRASS vector implementation and in particular of the geometry-database link. Therefore the writing of the `v.perp.seek` module and the general setup of the procedure has taken longer than it would today, with a more mature GRASS vector implementation and a more complete documentation.

The performance comparison between raster and vector approaches with respect to computational weight for the determination of the parameters on a regular domain awards the raster approach, since the higher computational cost is associated to the determination of the point on the surface though the point along its normal direction. Infact, the raster approach allows to store in memory the result of the adjoining cell, which can be used as start point for the search on the next voxel. The assumption that two successive points during

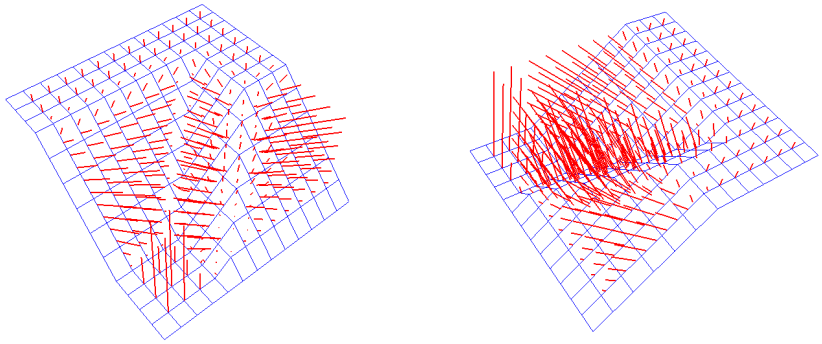

Figure 7: Two views of the DTM and of the normal segments from the centers of the voxels above the surface.

the elaboration are near does not hold for the vector approach: it is therefore unavoidable to start with wider "search window" (see section 4). This results in longer elaboration times and higher memory demand.

On the other hand the vector approach, with DBMS attribute management, allows great flexibility in the definition and manipulation of attribute and geometry. Attribute management benefits from all the tools available using a DBMS, since both input and output of the model can be fully expressed as database tables. Geometry flexibility is the most evident advantage of the vector model, allowing the evaluation of the parameters in a single point or on irregular sets of point. A typical choice is the use of irregular grids of points, with more dense points near the terrain surface and more sparse points far from it.

In conclusion, for regular domains the raster approach, showing better computational performance, is preferable, while for irregular set of points, or if attributes are stored in a database, the vector approach is a better choice.

9 Conclusions

The new GRASS vector model, its implementation and database connection constitute a powerful environment for the setup of physical models in 3D domains. The choice between vector and raster approach depends on the model and on the geometry involved, as seen on section 8. The value added by the development of a local atmospheric model in a GIS context lies in the availability of a proper environment for the management of referenced information and in the possibility of integrating the model's results in a broader environmental model. GRASS modules, such as `r.sun` and `r.slope.aspect`, are very useful to build maps that constitute intermediate results which are fed to the model.

The future developments of the atmospheric model include the evaluation of other parameters and a more sophisticated modeling of the influence of the land cover on sensible heat fluxes.

From the GIS point of view, apart from a general optimization of the algorithms, the attribute management through a DBMS still needs some work and the whole procedure must be made automatic though scripting to make the model available to non GIS specialists.

References

[1] Ciolli M., de Franceschi M., Rea R., Vitti A., Zardi D. and Zatelli P. Development and application of 2D and 3D GRASS modules for simulation of thermally driven slope winds. *Transactions in GIS*, 8(2), pages 191-209, 2004.

[2] Zatelli P., Ciolli M., Zardi D., De Franceschi M. and Rea R. Modeling of evaporation processes over tilted slopes by means of 3D GRASS raster. In Ciolli M. and Zatelli P., eds., *Open Source Free Software GIS - GRASS users conference 2002*, Trento, 11-13 september 2002.

Constant	Numeric value	measure unit
α	42.5	$[^o]$
g	980.6	$[cm^2 s^{-1}]$
B	0.4/100 m	$[^oC\,m^{-1}]$
	4×10^{-5}	$[^oC\,cm^{-1}]$
β	1/283	$[K]$
$\rho(0m)$	1.225×10^{-3}	$[g\,cm^{-3}]$
$\rho(20000m)$	0.09540×10^{-3}	$[g\,cm^{-3}]$

Parameter	Numeric value	measure unit
C	3.4	[^{o}C] ascensional flows
C	-2.1	[^{o}C] descendent flows
A	22.25	[^{o}C]
ℓ	34.37	$[m]$
Γ	0.004	$[^oC\,m^{-1}]$
$C\sqrt{\frac{g\beta\nu_H}{\Gamma\nu_k}}$	11.82	$[m\,s^{-1}]$ ascensional flows
$C\sqrt{\frac{g\beta\nu_H}{\Gamma\nu_k}}$	-0.715	$[m\,s^{-1}]$ descendent flows

Table 3: Constants and parameters used by Defant in [5].

[3] Zatelli P., Ciolli M., Zardi D. and Vitti A. 2D/3D grass modules use and development for atmospheric modeling. In Ciolli M. and Zatelli P., eds., *Open Source Free Software GIS - GRASS users conference 2002*, Trento, 11-13 september 2002.

[4] De Franceschi M., Rampanelli G., Sguerso D., Zardi D. and Zatelli P. Development of a measurement platform on a light airplane and analysis of airborne measurements in the atmospheric boundary layer. *Annals of geophysics*, 46(2), pages 269-283, 2003.

[5] Defant F. Zur theorie der Hangwinde, nebst Bemerkungen zur Theorie der Berg- und Talwinde. Archiv fuer Meteorologie Geophysik und Bioklimatologie Ser. A, 1: 421-450, 1949.

[6] Prandtl L. Führer durch die Strömungslehre. Braunschweigh Vieweg und Sohn, 1942

[7] Whiteman C. D. Observation of Thermally Developed Wind Systems in Mountain Terrain Atmospheric Processes over Complex Terrain. Amer. Meteor. Soc. Monographs (W. Blumen Ed.) 23: 5-42, 1990.

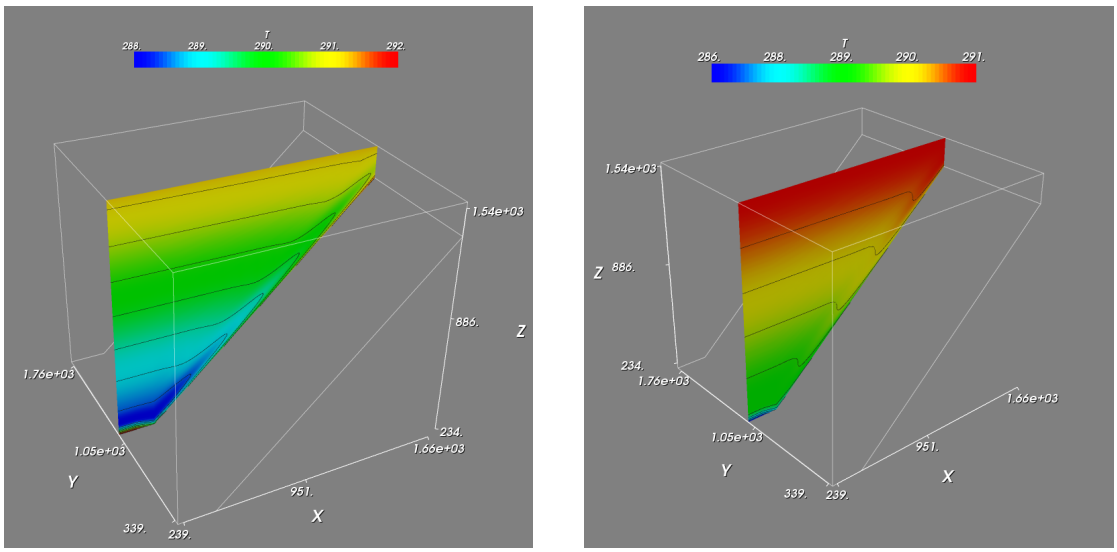

Figure 8: Output of the model for the Defant's parameters set: day (left) and night (right) temperature [k] distribution along the slope.

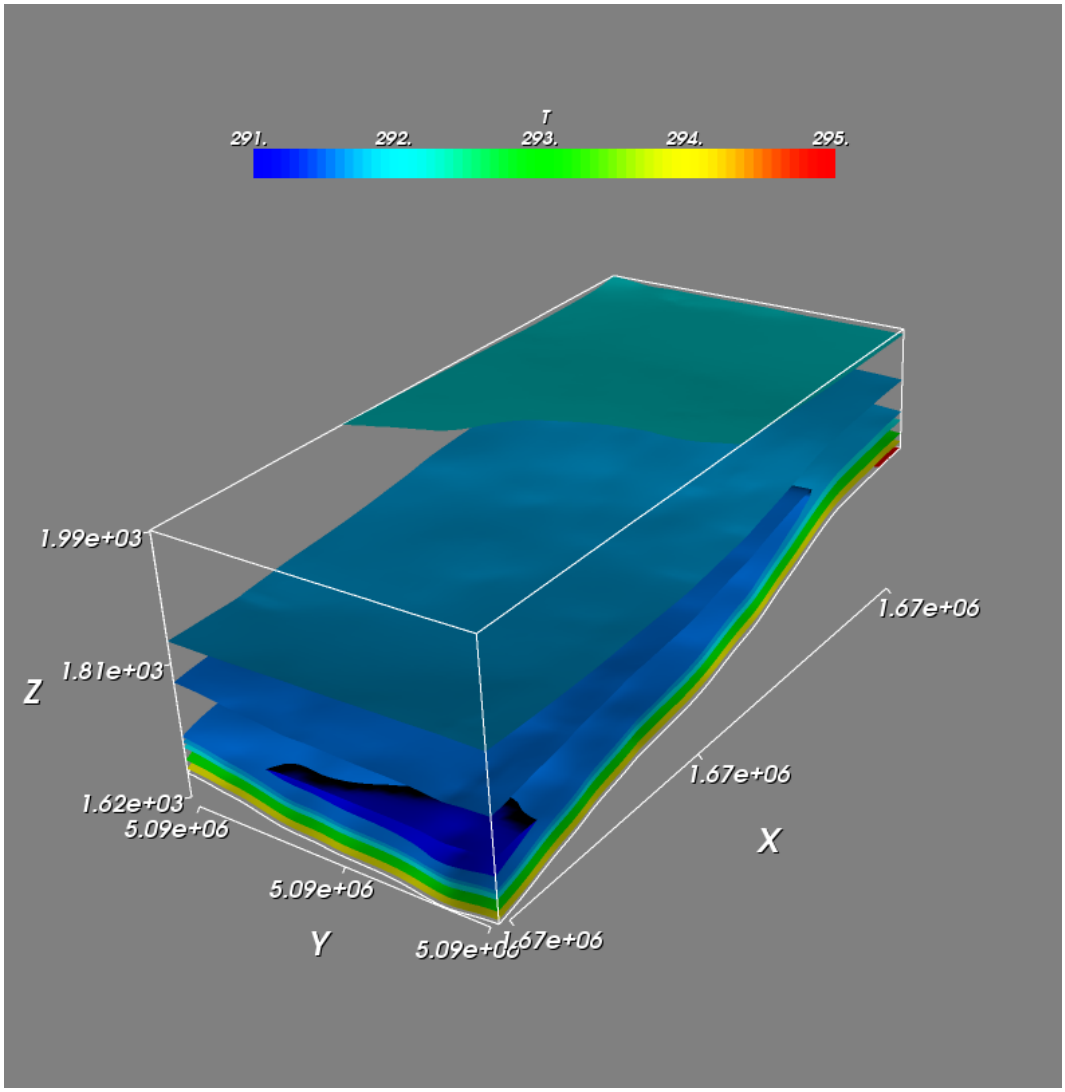

Figure 9: Temperature $[k]$ distribution on the slope near Besenello during the day.

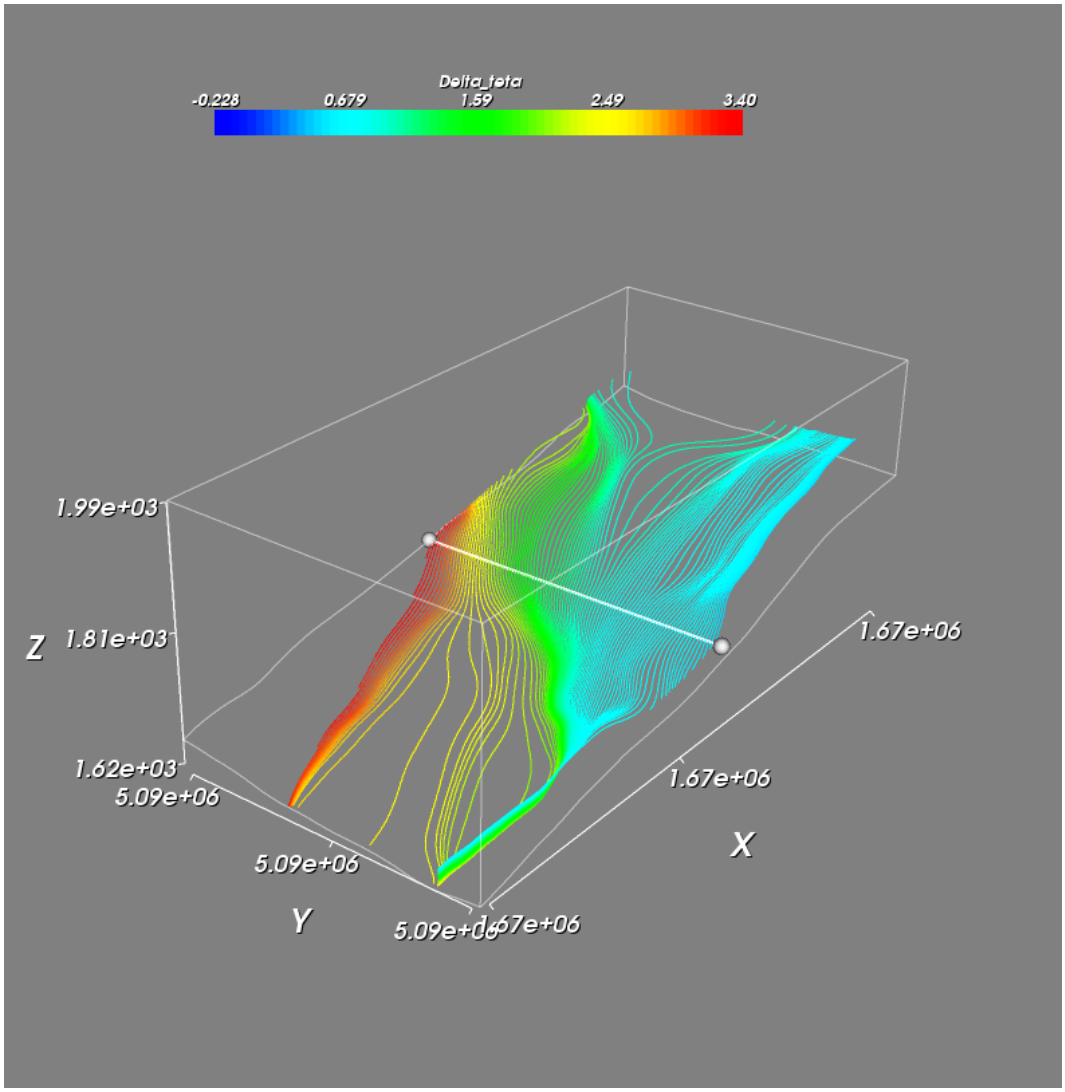

Figure 10: Potential temperature anomaly $[k]$ distribution on the slope near Besenello during the day.

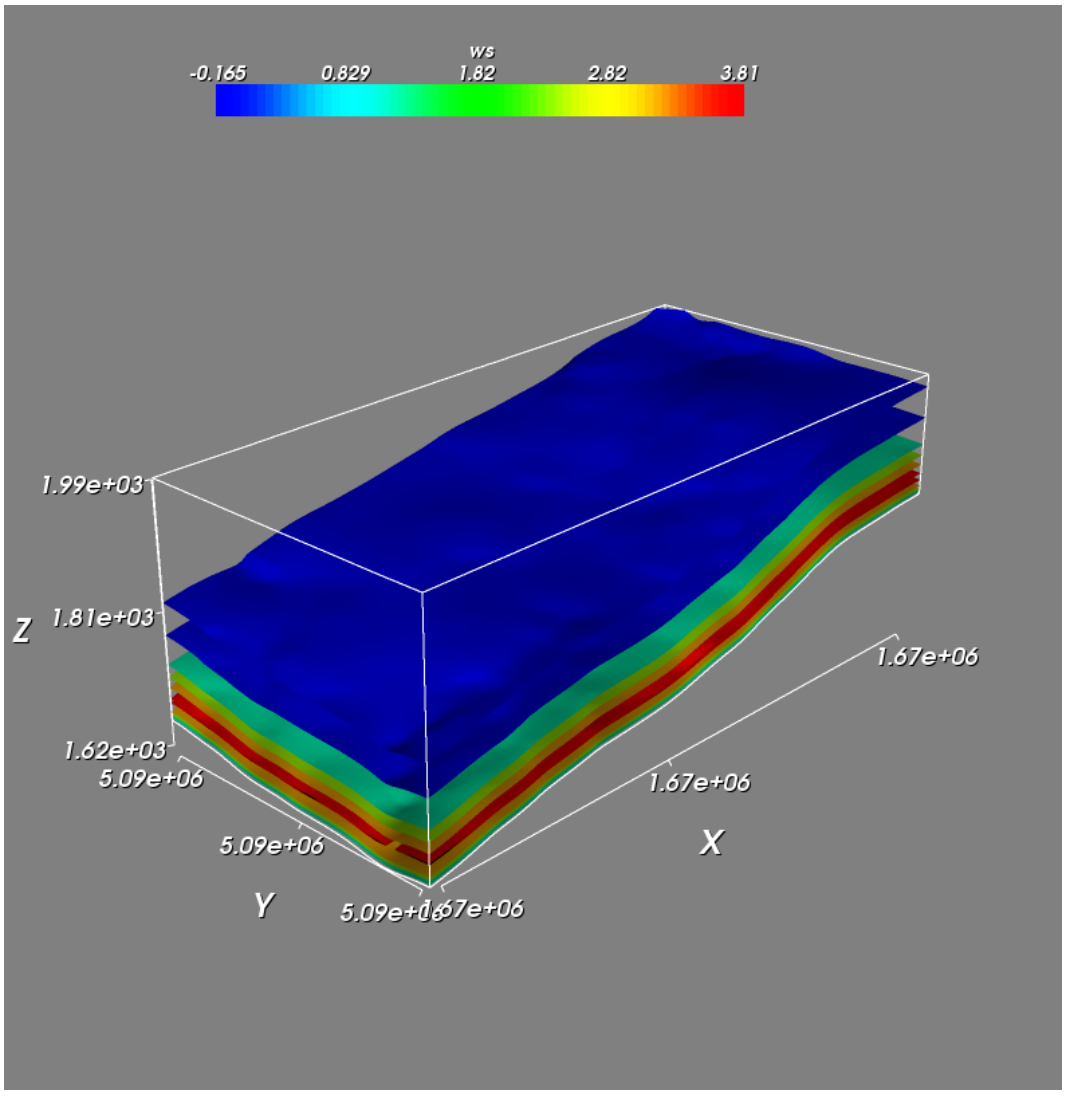

Figure 11: Wind velocity $[ms^{-1}]$ along the slope (here indicated as wind speed *ws*) near Besenello during the day.

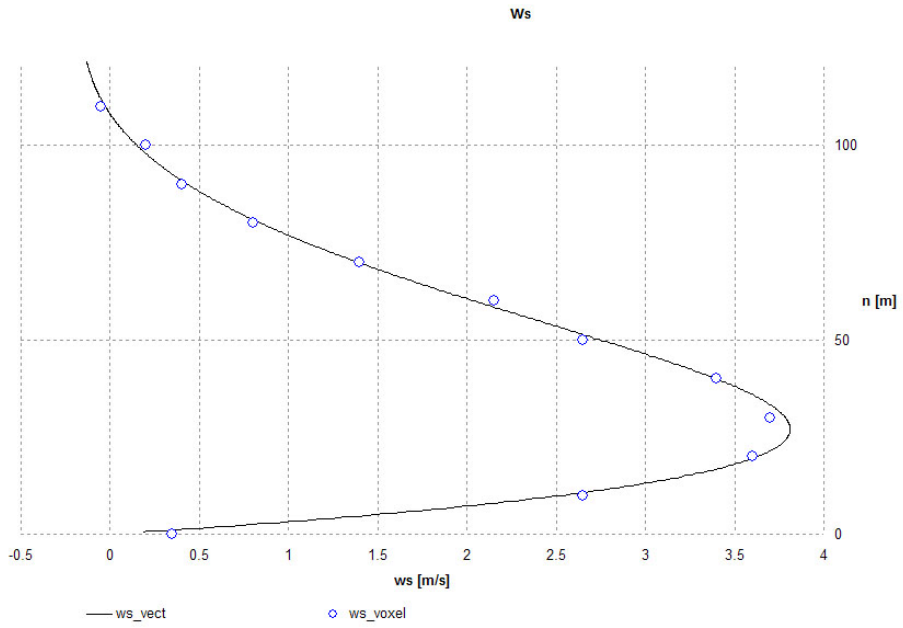

Figure 12: Comparison of the wind velocity along the slope (here indicated as *ws*) near Besenello during the day for the vector (ws_vector) and raster (ws_voxel) approach .

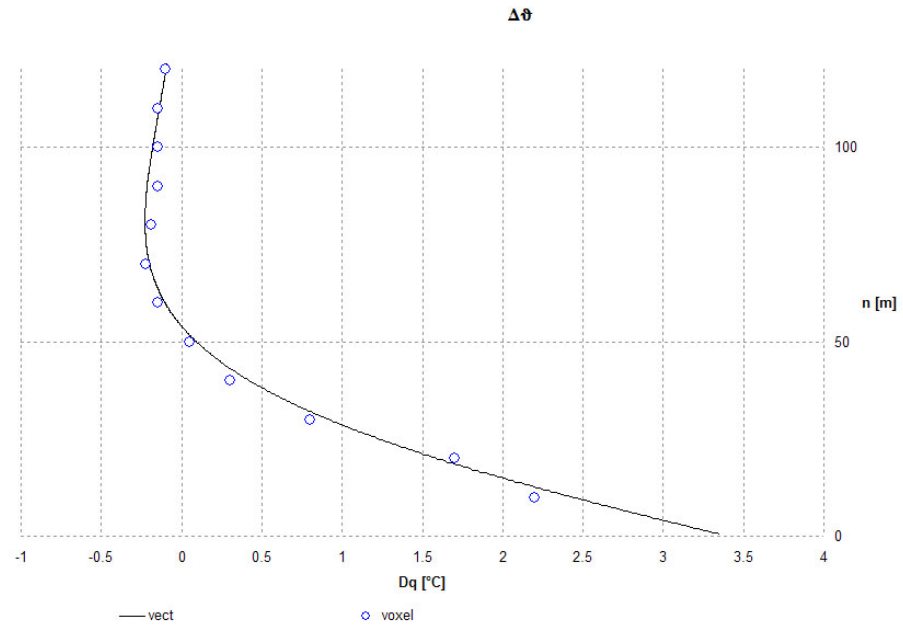

Figure 13: Comparison of the potential temperature anomaly $[k]$ along the slope near Besenello during the day for the vector (vect) and raster (voxel) approach .